A new tomographic-petrological model for the Ligurian-Provence back-arc basin (North-Western Mediterranean Sea)

Louise Boschetti, S Schwartz, Y Rolland, T Dumont, A Nouibat

Version of Record: https://www.sciencedirect.com/science/article/pii/S0040195123004092
Manuscript_2e83dae21d0e00a52344e76a89741ed9

A new tomographic-petrological model for the Ligurian-Provence back-arc basin (north-western Mediterranean Sea)

Boschetti, L.[1,2], Schwartz, S.[2], Rolland, Y.[2,4], Dumont, T.[2], Nouibat, A.[2,3]

1. Geosciences Environnement Toulouse, Université de Toulouse Paul Sabatier, CNRS, IRD, 14 av. Edouard Belin, 31400Toulouse, France
2. ISTerre, Université Grenoble Alpes, Univ. Savoie Mont Blanc, CNRS, IRD, IFSTTAR, 38000 Grenoble, France.
3. ITES, Institut Terre Environnement de Strasbourg, CNRS Université de Strasbourg, 67084 Strasbourg, France
4. EDYTEM, Université Savoie Mont Blanc, CNRS, UMR 5204, Le Bourget du Lac, France.

Abstract:

The nature of the crystalline basement of the Ligurian-Provence back-arc (LPB) basin is a matter debate as it remains unexplored by direct drilling methods. Several models have been proposed for the lower crustal structure comprising hyperextended continental crust or serpentinized mantle. In this paper, a new Vp-Vs geophysical dataset and corresponding tomography are used to propose a new petrological model for the LPB basin and for the formation of the crust of this back-arc domain. By crossing values of Vp, Vs and Vp/Vs ratios, the Messinian salt layer can be clearly identified down to 5 km depth, which highlights salt diapir structures into its overlying sedimentary cover. The 7.5 km depth corresponds to the transition with a heterogeneous basaltic oceanic crust about 4.5-5 km thick, intruded by rounded felsic gabbro plutons and underplated by a more mafic/ultramafic gabbro. This latter results from fractional crystallization of a hydrous magma inherited from the melting of a supra-subduction mantle which interacted with fluids originating from the subducting Adria slab. These magmas can be traced at the surface by magnetic anomalies punctuating the studied profile. Those new data and observations lead to conclude that the crust of the LPB basin resulted from a fast oceanic accretion during the opening of the back-arc. Its nature remains comparable to an immature oceanic crust with an overall basaltic and gabbroic composition and appears devoid of any serpentinized exhumed mantle.

Key words: back-arc basin, tomography, petrology, oceanic crust, Ligurian-Provence basin

Introduction

The precise description of the petrological nature of deep lithologies in oceanic domains is not straightforward it requires laboratory measurements (geochemical, rheological, petrophysical) on rocks extracted by drilling (e.g., Bonatti et al., 1990; Wilson et al., 2006; Larsen et al., 2018). Therefore, indirect geophysical methods designed to probe deep structures, such as seismic tomography, are needed (e.g., White et al., 1992; Grevemeyer et al., 2018). This is the case of the

Corresponding author:
E-mail address: louise.boschetti@get.omp.eu (L.Boschetti)

Ligurian-Provence basin (LPB) in the northwestern Mediterranean Sea where the crust still remains unexplored due to its thick sediment cover (5-8 km thick) (e.g., Gailler et al., 2009; Leprêtre et al., 2013).

Since the Late Cretaceous times, the geodynamic evolution of the western part of the Mediterranean domain has been controlled by the northward African plate motion relative to Europe (~1cm/y, e.g., Macchiavelli et al., 2017; Rosenbaum et al., 2002). This movement has led to several compressive and collisional events between Europe and micro-plates as Adria and Iberia (Fig. 1). These events resulted into the formation of mountain ranges all around the western Mediterranean Sea: the Alps, Apennines, Pyrenees, Betics and Dinarides (e.g., Romagny et al., 2020; Van Hinsbergen et al., 2020; Angrand and Mouthereau, 2021). Part of this convergence was also associated with the opening of several back-arc basins as the LPB, the Tyrrhenian, the Algerian and the Alboran basins, formed in response of slab retreat processes (e.g., Jolivet and Faccenna, 2000; Jolivet al., 2020). The characterization of the oldest one, the LPB, is complicated as it includes a thick sedimentary cover highlighted by seismic refraction and reflection, preventing any drilling down to the crust (e.g., Egger et al., 1988; Rollet et al., 2002; Dannowski et al., 2020). If the geological structure and the geodynamic of the basin have been well constrained (e.g., Chamot-Rooke et al., 1999; Séranne, 1999; Rollet et al., 2002), the petrological and lithological nature of the crustal basement is still debated and several hypotheses have been proposed: (1) a hyper extended margin that led to a very thin continental crust (e.g., Pascal et al., 1993, Dannowski et al., 2020); (2) a thin oceanic crust composed of tholeiitic volcanic rocks that cover directly the mantle, as it has been observed in several domains of the Tyrrhenian basin (e.g., Mascle and Réhault., 1990; Bonatti et al., 1990); (3) partly serpentinized peridotites of exhumed upper mantle, mostly devoid of volcanic crust (e.g., Gailler et al., 2009; Rollet et al., 2002; Moulin et al., 2015; Jolivet et al., 2020) also observed in the Tyrrhenian basin (e.g., Prada et al., 2014, 2015); (4) Lower crust partly intruded with magmatic material (Moulin et al.,2015).

Taking advantage of the availability of recent high-resolution Vp and Vs models (Dannowski et al., 2020; Nouibat et al., 2023), the purpose of the present paper is to further contribute in the description of the lithological and petrological nature of the crust beneath the oceanic domain of the LPB. Before the deployment of the Ocean-Bottom-Seismometers (OBS) (Fig. 2a) in the Ligurian Sea in 2017, the LPB was poorly described (e.g., Wolf et al., 2021; Nouibat et al., 2022a, 2022b). A unique opportunity is thus provided by the availability of these two new Vp and Vs seismological models to provide further insights into basin crust nature and structure. Indeed, the joint interpretation of Vp and Vs is crucial to discriminate the petrological nature of lithologies, since two lithologies of different petrological natures may have similar Vp and/or Vs signatures (e.g.,

67 Carlson et al., 1997; Christensen et al., 2004; Reynard, 2013; Grevemeyer et al., 2018; Malusà et
68 al., 2021).

69 Thus, in this paper, we first describe the different geological layers and lithologies that compose
70 the crust and the upper mantle of the LPB oceanic domain. Then, we discuss the significance of
71 data within the LPB context for the evolution of western Mediterranean crust that finally allow us to
72 propose a new petrological model for the LPB crust.

73 1. Geological setting of the Ligurian-Provence basin

74 The opening of the LPB was initiated 30 Ma ago by a rifting phase between European and Corsica-
75 Sardinia domains, following the back-arc extension above the north-westward subduction of Adria
76 micro-plate oceanic crust (e.g., Gattacceca et al., 2007; Jolivet al., 2020). The progressive south-
77 eastward roll-back and retreat of the Adria slab below the Corsica-Sardinia domain led to
78 continental crust stretching followed by continental break-up during Early Miocene, and to the
79 genesis of an oceanic crust domain between 20 and 15 Ma (Pascal et al., 1993; Contrucci et al.,
80 2001; Rollet et al., 2002). As a result, the LPB comprises two conjugated thinned continental
81 passive margins separated by an oceanic domain in its central part (Fig. 2a). The entire basin is
82 characterized by magnetic anomalies interpreted as magmatic bodies identified from acoustic
83 facies in seismic reflection profiles (Rollet et al., 2002). The area between margins and the oceanic
84 domain corresponds to a transition zone likely made up of a very thin continental crust overlying a
85 thick rift-related magmatic underplating corner (e.g., Séranne, 1999; Rollet et al., 2002). This limit
86 is marked by an abrupt change in the amplitude of magnetic anomalies featured by the passage
87 from mostly positive values in the deep (i.e., oceanic) basin, to negative values at the Continent-
88 Ocean Transition and by a change in acoustic facies seen on seismic reflection data (e.g., Réhault
89 et al., 1984; Rollet et al., 2002). The nature of magmatic bodies from sampled rocks occurring in
90 the margins has been shown to have a tholeiitic nature, with a back-arc affinity as shown by a
91 strong subduction component (e.g., Réhault et al., 2012 and references therein). However, the
92 nature of magmatism observed in this oceanic domain could not be studied from direct petro-
93 geochemical analyses unlike contexts where the crust is accessible by dragging or drilling (e.g.,
94 Falloon et al., 1992; Wilson et al., 2006) and is thus still debated.

95 A stratigraphic log representative of the Ligurian Basin has been built (Fig. 2b) based on units
96 identified from combined wide angle and reflection seismic data (Klingelhoefer et al., 2008; Gailler
97 al., 2008; Leprêtre et al., 2013; Dannowski et al., 2020). These data reveal a sedimentary layer of
98 5 km average thickness and P-waves velocities ranging between 1.9 and 5 km/s. This layer is
99 made up of Plio-Quaternary sediments, Messinian and pre-salt units. The Plio-Quaternary to
100 Messinian unit transition is marked by a velocity of ~2.5 km/s. The Messinian sequence exhibits

strong variations in thickness ascribed to salt diapirism and is separated from a pre-salt unit by the 4.2 km/s contour. Lower sediments overly an oceanic basement, marked by the 5 km/s contour. The crust is relatively thin and exhibits an average thickness of 4.5 km. Crustal P-wave velocities range from 5 to 7.2-7.3 km/s at ~12 km depth, which corresponds to the transition with the Upper Mantle (Vp > 7.3 km/s). Although these data allow to constrain the thicknesses of main layers and location of major interfaces (intra-sedimentary, sediment-crust and Moho), they only rely on P-waves velocities. Consequently, in the absence of available S-wave velocities, they did not allow to reliably constrain the petrological nature of crust, which remains a matter of debate as a typical or atypical oceanic crust with the presence of domains of exhumed serpentinized mantle (Rollet et al., 2002; Klingelhoefer et al., 2008; Gailler al., 2008; Leprêtre et al., 2013) or as a hyperextended continental crust (Dannowski et al., 2020).

2. Seismic cross section of the central oceanic domain

The 3D Vs model by Nouibat et al., (2023) covers the Ligurian-Provence basin and goes down to 100 km depth. This model has been derived using wave-equation tomography of ambient noise data recorded by the OBSs of the AlpArray temporary network (Hetényi et al., 2018) and land stations from European permanent networks available in the period 2015-2019 (Nouibat et al., 2023 and reference therein) (Figure 1). This model is an improved version of the Nouibat et al., (2022b) model and this is the most consistent available Vs model of the LPB since it accounts for the 3D effects of the water layer on the wave propagation of ambient-noise surface waves. Indeed, Nouibat et al., (2023) have considered the 3D fluid/solid coupling in the Ligurian sea for their wave equation tomography. The Vp model by Dannowski et al. (2020) has been derived using high-resolution P-wave travel time tomography of active-seismic refraction data recorded by OBSs and ocean-bottom hydrophones (OBHs) along a 127.5 km profile in the axis of LPB (LOBTSER-P02; Fig. 2). This model goes down to ~ 15 km as a maximum depth, with a high-resolution coverage of the crust at the illuminated part of the uppermost mantle. Additionally, we use the probabilistic model of Nouibat et al. (2022b) to estimate depths and geometries of limits between geological layers. This model is obtained by 1D Bayesian inversion in depth that allow to estimate the probability to have lithological interfaces at each location and each depth. Those interfaces probabilities cannot be estimated with the model of Nouibat et al., (2023) as the inversion method used is not the same.

This discussion focuses on the portion of LPB following the LOBTSER-P02 profile where Vp is defined. Figures 3a-b show the 2D cross-sections of the probability of interfaces and Vs computed along the same profile, and the Vp section from Dannowski et al. (2020). We are aware that these Vp and Vs models have different resolutions and different sensitivities as they are obtained from

different datasets, with different imaging techniques. In both imaging techniques, uncertainties are not well constrained as they are not processed during inversions. For this reason, we cannot give estimates. However, we do have an estimate of the lateral and vertical resolutions of the two models: ~ 5 to 10 km laterally / ~ 1 to 3 km vertically for the Vs model (Nouibat et al., 2023), and ~ 2.5 to 5 km laterally / ~ 0.5 to 1.5 km vertically for Vp (Dannowski et al., 2020). The Vs model is smoother since it is derived from surface waves. However, it remains pertinent in recovering first-order 3D velocity structures of the crust given the high-sensitivity of ambient-noise surface waves to the 3D lateral variations (e.g., Shapiro et al., 2005; Stehly et al., 2009; Molinari et al., 2015). For the above-mentioned point, the interpretation of the crust petrological nature and its different lithologies, relies on joint point-by-point division of the two models, Vs and Vp absolute values and comparisons with Vp and Vs ranges of different rock type fiels deduced from Grevemeyer et al., (2018) study. Then a Vp/Vs ratio imaging of the section is used to illustrate our results.

This method allows us to identify four main layers presented above (Fig. 3):

(1) The deepest interface probability, located at 12 km marks the crust-mantle transition and matches the depth of the velocity contour with Vs = 4.1 km/s and Vp = 7.2 km/s. Those values correspond to an oceanic crust as defined by Grevemeyer et al. (2018) from Vp and Vs acquisition along off-axis profiles of older oceanic lithosphere at Mid-Cayman Spreading Centre.

(2) The intermediate interface occurs near 7.5 km depth, which coincides quite well with the velocity contour Vs = 3.2 km/s and corresponds to a Vp contour of 4-4.1 km/s. This contour is also observed with multichannel seismic data (MCS) and defined as a crystalline basement (Dannowski et al., (2020). Thus, it can be considered as the sediment-oceanic crust transition.

(3) A shallower and relatively pronounced interface, with rather high interface probabilities, occurs at about 5 km depth. This interface is in good correspondence with the depth of the velocity contour Vs = 2.3 km/s and Vp = 4.2 km/s. Theses values are coherent with salt velocities from Yan et al., (2016). Moreover, through MCS data, Dannowski et al., (2020) interpreted a salt layer with diapiric structues between 4-6 km. The same interpretation is proposed by Contrucci et al., (2001) in our study area with a diapir layer base at a depth of 5.7 km and thikness around 1.7 km. Those observations are coherent with our data.

(4) In the Vp section, toward the base of oceanic crust on both sides of transect, we note the presence of discontinuous domains with high velocity anomalies (Vp = 6-7.2 km/s, in green on Fig. 3c) with respect to the rest of the oceanic crust, which exhibit a weaker Vp gradient at the Moho. These anomalies correspond to Vs between 4 and 4.4 km/s.

These first order observations allow defining a first layer of Messinian salt deposit of about 2.5 km exhibiting significant variations in thickness (locally up to 5 km), then a sediment layer of about 2.5 km (between 5 and 7.5 km) and finally between sediments and the mantle, an oceanic crust with a thickness ranging from 4.5 to 5 km (between 7.5 and 12 km depth). The mantle could also be considered in the model as a layer with Vp higher than 7.2 km/s and Vs higher than 4.1 km/s.

3. Insights for the petrological nature of the oceanic domain

In this section, we further discuss the petrological nature of the crust and upper mantle of the LPB (Fig. 4). This discussion is based on the seismic data (Vp, Vs) available along a reference cross section in the oceanic LPB domain (Dannowski et al., 2020; Nouibat et al., 2023). These data are discussed in the light of the Vp vs Vs diagram which defined different lithology filed for the oceanic crust (Grevemeyer et al., 2018). These fields are deduced from studies using different seismic profiles crossing the well-known Mid-Cayman Spreading Centre, where the estimated RMS error ranges from ~0.02 km/s to ~0.5 km/s on the Vp and Vs data of one of the seismic line used, and with RMS error roughly ranging from 0.005 to 0.17 on the Vp/Vs ratio along the same profile (P05 in Grevemeyer et al., 2018). We first note that the oceanic crust is dominated by rocks with a seismic signature of basalts with low hydrothermal alteration. This is confirmed by the value of Vp/Vs ratio ranging from 1.5 to 1.6 km/s (Fig. 4c). Thus, we suggest that the oceanic crust is mainly formed by basaltic lava flows (BLF) (Fig. 4a, b). At both section extremities, we identified bodies with distinct Vp values (Fig. 4c). These bodies exhibit the same Vp/Vs ratio as the crust, but absolute value data from Vs and Vp are largely higher. These values correspond to those of gabbros with a crustal affinity (IGc) due to their position at the transition between basalt and gabbro fields (Fig. 4a).

The mantle also exhibits a heterogeneous seismic signature. In the area where the Vp/Vs ratio range between 1.7 and 1.9, these values are similar to an anhydrous peridotite mantle (M in Fig. 4a). Further, an elongate shape domain with values at the upper boundary of gabbros (“mantle affinity” gabbroic bodies or IGm), with higher Vp/Vs ratio than IGc is also observed (Fig. 4b). The difference between IGc and IGm can be explained by fractional crystallization of a hydrous magma formed in the back-arc with a strong metasomatic influence from the subducting slab. Such magmas show a differentiation during fractional crystallization in hydrous conditions leading to a first phase of crystallization of olivine and pyroxene instead of plagioclase (e.g., Gaetani et al., 1994; Arai et al., 2014). This can form IGm plutonic bodies with a mafic/ultramafic composition resulting in olivine and pyroxene accumulation at the base of the pluton (olivine-rich cumulate layer in Fig. 4b; e.g., Müntener et al., 2001; Arai et al., 2014). As a result of this first differentiation phase in the pluton upper part, the fractional crystallization leads to a marked “crustal affinity” (IGc) of the

gabbroic pluton that can present amphibole cumulates instead of pyroxene (e.g., Müntener et al., 2001; Cleason et al., 2004). These gabbroic bodies are located at the base of the crust and are interpreted as having a more felsic (plagioclase-rich) mineralogical composition (e.g., Nicholls and Ringwood, 1973; Arai et al., 2014). Their formation could be associated with dolerite dykes and sills located at the upper part of the gabbroic pluton, and may correspond to the central emission of the BLFs as is commonly observed in relatively immature-spreading ridges (Fig. 4b) (e.g., Saunders et al., 1982; Janoušek et al., 2013; Terinha et al., 2018). This kind of magmatism is consistent with the back-arc volcanism observed in both margins with dolerite dykes of K-calc-alkaline basalts formed during Miocene times in Corsica and Sardinia and alkaline basalts found in Southern France (Toulon area; Réhault et al., 2012 and references therein). Further, several magnetic anomalies have been described in the LPB (Rollet et al., 2002). Their superimposition with volcanic/magmatic bodies localisation determined by seismic facies allowed Rollet et al., (2002) to propose a correlation between both anomalies and volcanic/magmatic bodies. After superimposition of our seismic Vs/Vp transect on the magnetic map of Rollet et al., (2022), we suggest that in our domain, magnetic anomalies could correspond to gabbroic bodies as they appear to be correlated with their emplacement in the geophysical tomography (Fig. 4c). This observation could appear counter-intuitive with an oceanic crust interpretation because gabbros generally present a lower magnetisation than basalts. Further, in our case, there are no linear magnetic anomalies in the BLF as it is normally seen in a mature oceanic crust (Bayer et al., 1973; Sandwell and Smith, 1997; Rollet et al., 2002). However, we explain this peculiar magnetic signal of oceanic crust as (i) due to the fluid-rich fractionation of the gabbros producing crystallization of large amounts of magnetite and thus to a higher magnetic signal (e.g., Claeson et al., 2004). Furthermore (ii), the lack of linear anomalies in BLFs suggests a rather immature stage of ridge magmatism with a rather radial dispersion of lavas emitted from IGc bodies, and possible slight alteration of the lavas, especially during the Messinian phase, which may have altered the magnetic minerals and led to a demagnetization of basalts. Moreover, recent studies show that even in a mature oceanic crust, magnetisation of gabbro layers cannot be ignored with an impact to the magnetic anomalies of up to 10%-30% (Hu et al., 2023). It means that magnetic anomalies seen in the LPB could have a gabbroic origin instead of a serpentinite one, as it has been discussed previously (e.g., Gailler et al., 2009; Moulin et al., 2015; Jolivet et al., 2020). Moreover, our seismic observations show no evidence of any serpentinized mantle, which would rather show Vp/Vs ratios higher than 1.9 (Fig. 4a). In the same way, no hydration of the crust is observed, as its Vp/Vs ratio is higher than 1.5. Finally, the presence of a minimum 4.5 km basaltic crust thickness excludes the hypothesis of a hyperextended continental crust basement (Dannowski et al., 2020) for the Ligurian-Provence central domain.

Here, we propose a new petrological model for the LPB crust (Fig. 4b) for a transect of the central part of the LPB where Vp and Vs are available, which is ideally chosen to decipher the structure of the oceanic crust far from the 'transition zones' to the continental crust. This petrological model shows:

(1) a relatively thin (4.5 km) oceanic crust formed by basaltic lava flows, cross-cut by bodies of intrusive gabbros emplaced at different levels: (i) below the base of the crust as large underplated mafic/utlramafic gabbroic bodies, (ii) within the lower part of the BLF crust as more felsic gabbroic bodies (IGc).

(2) The underlying mantle appears devoid of any serpentinization, indicating that is has never undergone significant hydrothermal alteration and was therefore never exposed to the seafloor surface. This observation is coherent with the geodynamic context, as the Ligurian-Provence basin appears to have formed at relatively fast accretion, associated with a back-arc extension rate estimated superior to 3 cm/yr (Faccenna et al., 1997; Séranne et al., 1999; Chamot-Rooke et al., 1999).

More evolved back-arc basins as the Grenada basin present the same kind of crust as the LPB with a 6-8 km thick basaltic crust superimposed on a mantle devoid of any serpentinization (Allen et al., 2021, Padron et al., 2021). In the same way, the Lau back-arc basin (Pacific Ocean) shows a similar order of basaltic crust thickness, and is also featured by intrusive felsic gabbroic bodies and underplated mafic gabbroic bodies that support our observation in the LPB (Arai et al., 2014). Thus, as exemplified in this study, the Vp/Vs ratio allows to better constrain the nature of the crust, including some specific petrological features in magmatic rocks and the morphology of sediment strata like the Messinian salt. This latter appears to have a typical diapiric shape, with a variable depth of the layer base, between 6.5 and 5 km, and a variable thickness about 0.5 and 2 km resulting from diapirism, as it has been observed in seismic reflection data by Contrucci et al. (2001) and Dannowski et al., (2020).

4. Conclusion

Geophysical data with Vp, Vs and Vp/Vs ratios allows an accurate imaging of the Ligurian-Provence back-arc basin, and a precise localisation of geological interfaces. Based on these data, an improved petrological model of the back-arc crust is proposed. Our model suggests a heterogeneous crust with thick sedimentary layers in which a diapiric salty interface can be observed very precisely at 5 km depth. Then, the oceanic crust is emphasized by relatively thick, 4.5-5 km, basaltic crust comprised of slightly altered lava

flows. This crust is punctuated by rounded intrusive felsic gabbroic bodies rooting down into the Moho and some underplated more mafic cumulative gabbros below the Moho. These melts were formed by the fractional crystallization of hydrous magmas which originated from the subducting slab, resulting in the fractionation of magnetite and amphibole. The geophysical signature of the mantle is similar to that of anhydrous peridotites. This oceanic crust structure is thought to represent an immature oceanic ridge, interpreted as resulting from a fast opening of the Ligurian back-arc basin. For these reasons, the Ligurian-Provence basin is devoid of any serpentinized mantle, as it was never exhumed and exposed at sea floor level.

Declaration of Competing Interest

The authors declare that they have no known competing financial interests or personal relationships that could have appeared to influence the work reported in this paper**.**

Acknowledgements

This work forms part of the PhD dissertation of the first author, funded by the French Ministry of Research and High Education and supported by SDU2E doctoral school (Toulouse Paul Sabatier University) and the RGF BRGM program. We warmly thank Anke Dannowski (GEOMAR Helmholtz Centre for Ocean Research Kiel) for providing us the P-wave velocity model of the LOBSTER-P02 transect. This paper benefit from constructive reviews by David Graindorge and an anonymous reviewer, and efficient editorial handling by Ramon Carbonell.

References

Allen, R. W., 2021. Shedding New Light on an Enigmatic End Member of Back-Arc Spreading: The Structure of the Grenada Basin in the Lesser Antilles. Journal of Geophysical Research: Solid Earth 126(3), e2021JB021649.

Angrand, P., Mouthereau, F., 2021. Evolution of the Alpine orogenic belts in the Western Mediterranean region as resolved by the kinematics of the Europe-Africa diffuse plate boundary. BSGF-Earth Sciences Bulletin 192(1), 42, https://doi.org/10.1051/bsgf/2021031.

Arai, R., Dunn, R. A., 2014. Seismological study of Lau back arc crust: Mantle water, magmatic differentiation, and a compositionally zoned basin. Earth and Planetary Science Letters 390, 304-317.

Bayer, R., Le Mouel, J. L., Le Pichon, X., 1973. Magnetic anomaly pattern in the western Mediterranean. Earth and Planetary Science Letters 19(2), 168-176.

Bonatti, E., Seyler, M., Channell, J., Girardeau, J., Mascle, G., 1990. Peridotites drilled from the Tyrrhenian Sea, ODP. In: Proc. Ocean Drill. Program Sci. Results 107, pp. 37-47.

303 Carlson, R. L., Miller, D. J., 1997. A new assessment of the abundance of serpentinite in the oceanic crust. Geophysical
304 Research Letters 24(4), 457-460.
305 Christensen, N. I., 2004. Serpentinites, peridotites, and seismology. International Geology Review 46(9), 795-816.
306 Claeson, D. T., Meurer, W. P., 2004. Fractional crystallization of hydrous basaltic “arc-type” magmas and the formation
307 of amphibole-bearing gabbroic cumulates. Contributions to Mineralogy and Petrology 147, 288-304.
308 Chamot-Rooke, N., Gaulier, J. M., Jestin, F., 1999. Constraints on Moho depth and crustal thickness in the Liguro-
309 Provençal basin from a 3D gravity inversion: geodynamic implications. Geological Society, London, Special
310 Publications, 156(1), 37-61.
311
312 Contrucci, I., Nercessian, A., Béthoux, N., Mauffret, A., Pascal, G., 2001. A Ligurian (western Mediterranean Sea)
313 geophysical transect revisited. Geophysical Journal International 146(1), 74-97.
314 Dannowski, A., Kopp, H., Grevemeyer, I., Lange, D., Thorwart, M., Bialas, J., Wollatz-Vogt, M., 2020. Seismic evidence
315 for failed rifting in the Ligurian Basin, Western Alpine domain. Solid Earth 11(3), 873-887.
316 Egger, A., Demartin, M., Ansorge, J., Banda, E., Maistrello, M., 1988. The gross structure of the crust under Corsica and
317 Sardinia. Tectonophysics 150(3), 363-389.
318 Faccenna, C., Piromallo, C., Crespo-Blanc, A., Jolivet, L., Rossetti, F., 2004. Lateral slab deformation and the origin of
319 the western Mediterranean arcs. Tectonics 23(1), https://doi.org/10.1029/2002TC001488
320 Faccenna, C., Mattei, M., Funiciello, R., Jolivet, L., 1997. Styles of back-arc extension in the central Mediterranean. Terra
321 Nova, 9(3), 126-130.
322 Falloon, T. J., Malahoff, A., Zonenshaina, L. P., Bogdanova, Y., 1992. Petrology and geochemistry of back-arc basin
323 basalts from Lau Basin spreading ridges at 15, 18 and 19 S. Mineralogy and Petrology 47, 1-35.
324 Gaetani, G. A., Grove, T. L., Bryan, W. B., 1994. Experimental phase relations of basaltic andesite from hole 839B under
325 hydrous and anhydrous conditions. In: Proceedings of the Ocean Drilling Program, scientific results 135, pp. 557-
326 563.
327 Gailler, A., Klingelhoefer, F., Beslier, M., Olivet, J., Aslanian, D., Bache, F., et al., 2008. First results from the SARDINIA
328 deep seismic cruise on the Western Sardinia and Gulf of Lions conjugate margin pair. In AGU Fall Meeting
329 Abstracts 2008, pp. T43C-2046.
330 Gailler, A., Klingelhoefer, F., Olivet, J. L., Aslanian, D., Technical, O. B. S., 2009. Crustal structure of a young margin
331 pair: New results across the Liguro–Provencal Basin from wide-angle seismic tomography. Earth and Planetary
332 Science Letters 286(1-2), 333-345.
333 Gattacceca, J., Deino, A., Rizzo, R., Jones, D. S., Henry, B., Beaudoin, B., Vadeboin, F., 2007. Miocene rotation of
334 Sardinia: New paleomagnetic and geochronological constraints and geodynamic implications. Earth and
335 Planetary Science Letters 258(3-4), 359-377.
336 Grevemeyer, I., Hayman, N. W., Peirce, C., Schwardt, M., Van Avendonk, H. J., Dannowski, A., & Papenberg, C. 2018.
337 Episodic magmatism and serpentinized mantle exhumation at an ultraslow-spreading centre. Nature Geoscience,
338 11(6), 444-448.
339 Hetényi, G., Molinari, I., Clinton, J., Bokelmann, G., Bondár, I., Crawford, W. C., et al., 2018. The AlpArray seismic
340 network: a large-scale European experiment to image the Alpine Orogen. Surveys in geophysics 39, 1009-1033.
341 Hu, Y., Zhang, J., Jiang, Z., Li, Y., Li, S., 2023. Influence of the oceanic crust structure on marine magnetic anomalies:
342 Review and forward modelling. Geological Journal 58(3), 1069-1082.
343 Janoušek, V., Aichler, J., Hanžl, P., Gerdes, A., Erban, V., Žáček, V., et al., 2014. Constraining genesis and geotectonic
344 setting of metavolcanic complexes: a multidisciplinary study of the Devonian Vrbno Group (Hrubý Jeseník Mts.,
345 Czech Republic). International Journal of Earth Sciences 103, 455-483.
346 Jolivet, L., Faccenna, C., 2000. Mediterranean extension and the Africa-Eurasia collision. Tectonics 19(6), 1095-1106.

347 Jolivet, L., Romagny, A., Gorini, C., Maillard, A., Thinon, I., Couëffé, R., et al., 2020. Fast dismantling of a mountain belt
348 by mantle flow: late-orogenic evolution of Pyrenees and Liguro-Provençal rifting. Tectonophysics 776, 228312.
349 Klingelhoefer, F., Olivet, J., Aslanian, D., Bache, F., Moulin, M., Matias, L., 2008. Preliminary results from the Sardinia
350 deep seismic cruise on the Western Sardinia and Gulf of Lions conjugate margin pair. In EGU Meeting,
351 2008AGUFM.T43C2046G.
352 Larsen, H. C., Mohn, G., Nirrengarten, M., Sun, Z., Stock, J., Jian, Z., ... & Zhong, L., 2018. Rapid
353 transition from continental breakup to igneous oceanic crust in the South China Sea. Nature Geoscience, 11(10),
354 782-789.
355 Leprêtre, A., Klingelhoefer, F., Graindorge, D., Schnurle, P., Beslier, M. O., Yelles, K., et al., 2013. Multiphased tectonic
356 evolution of the Central Algerian margin from combined wide-angle and reflection seismic data off Tipaza,
357 Algeria. Journal of Geophysical Research: Solid Earth, 118(8), 3899-3916.
358 Macchiavelli, C., Vergés, J., Schettino, A., Fernàndez, M., Turco, E., Casciello, E. et al. 2017. A new southern North
359 Atlantic isochron map: Insights into the drift of the Iberian plate since the Late Cretaceous. Journal of Geophysical
360 Research: Solid Earth 122(12), 9603-9626.
361 Malusà, M. G., Guillot, S., Zhao, L., Paul, A., Solarino, S., Dumont, T., Yuan, H., 2021. The deep structure of the Alps
362 based on the CIFALPS seismic experiment: A synthesis. Geochemistry Geophysics Geosystems 22(3),
363 e2020GC009466.
364 Mascle, J., Rehault, J. P., 1990. A revised seismic stratigraphy of the Tyrrhenian sea: implicationfor the basin evolution.
365 In: Proc. Ocean Drill. Program Sci. Results 107, pp. 617-636617-636.
366 Moulin, M., Klingelhoefer, F., Afilhado, A., Aslanian, D., Schnurle, P., Nouzé, H., Feld, A., 2015. Deep crustal structure
367 across a young passive margin from wide-angle and reflection seismic data (The SARDINIA Experiment)–I. Gulf
368 of Lion's margin. Bulletin de la Société géologique de France 186(4-5), 309-330.
369 Müntener, O., Kelemen, P. B., Grove, T. L., 2001. The role of H2O during crystallization of primitive arc magmas under
370 uppermost mantle conditions and genesis of igneous pyroxenites: an experimental study. Contributions to
371 Mineralogy and Petrology 141, 643-658.
372 Nicholls, I. A., Ringwood, A. E., 1973. Effect of water on olivine stability in tholeiites and the production of silica-saturated
373 magmas in the island-arc environment. The Journal of Geology 81(3), 285-300.
374 Nouibat, A., Brossier, R., Stehly, L., Cao, J., Paul, A., & Cifalps Team and AlpArray Working Group,. 2023. Ambient-
375 noise wave-equation tomography of the Alps and Ligurian-Provence basin. Journal of Geophysical Research:
376 Solid Earth, 128, e2023JB026776
377 Nouibat, A., Stehly, L., Paul, A., Schwartz, S., Rolland, Y., Dumont, T., et al., 2022b. Ambient-noise tomography of the
378 Ligurian-Provence Basin using the AlpArray onshore-offshore network: Insights for the oceanic domain
379 structure. Journal of Geophysical Research: Solid Earth, 127(8).
380 Nouibat, A., Stehly, L., Paul, A., Schwartz, S., Bodin, T., Dumont, T et al., 2022a. Lithospheric transdimensional ambient-
381 noise tomography of W-Europe: implications for crustal-scale geometry of the W-Alps. Geophysical Journal
382 InternationaCl 229(2), 862-879.
383 Pascal, G. P., Mauffret, A., Patriat, P., 1993. The ocean-continent boundary in the Gulf of Lion from analysis of
384 expanding spread profiles and gravity modelling. Geophysical Journal International 113(3), 701-726.
385 Padron, C., Klingelhoefer, F., Marcaillou, B., Lebrun, J. F., Lallemand, S., Garrocq, C., et al., 2021. Deep structure of the
386 Grenada Basin from wide-angle seismic, bathymetric and gravity data. Journal of Geophysical Research: Solid
387 Earth 126(2), e2020JB020472.
388 Prada, M., Sallarès, V., Ranero, C. R., Vendrell, M. G., Grevemeyer, I., Zitellini, N., de Franco, R., 2014. Seismic
389 structure of the Central Tyrrhenian basin: Geophysical constraints on the nature of the main crustal domains.
390 Journal of Geophysical Research: Solid Earth 119(1), 52-70.

Prada, M., Sallarès, V., Ranero, C. R., Vendrell, M. G., Grevemeyer, I., Zitellini, N., de Franco, R., 2015. The complex 3-D transition from continental crust to backarc magmatism and exhumed mantle in the Central Tyrrhenian basin. Geophysical Journal International 203(1), 63-78.

Rehault, J. P., Boillot, G., Mauffret, A., 1984. The western Mediterranean basin geological evolution. Marine Geology 55(3-4), 447-477.

Réhault, J. P., Honthaas, C., Guennoc, P., Bellon, H., Ruffet, G., Cotten, J., et al., 2012. Offshore Oligo-Miocene volcanic fields within the Corsica-Liguria Basin: Magmatic diversity and slab evolution in the western Mediterranean Sea. Journal of Geodynamics 58, 73-95.

Reynard, B., 2013. Serpentine in active subduction zones. Lithos 178, 171-185.

Romagny, A., Jolivet, L., Menant, A., Bessière, E., Maillard, A., Canva, A., et al., 2020. Detailed tectonic reconstructions of the Western Mediterranean region for the last 35 Ma, insights on driving mechanisms. Bulletin de la Société géologique de France 191(1).

Rollet, N., Déverchère, J., Beslier, M. O., Guennoc, P., Réhault, J. P., Sosson, M., Truffert, C., 2002. Back arc extension, tectonic inheritance, and volcanism in the Ligurian Sea, Western Mediterranean. Tectonics, 21(3), 6-1.

Rosenbaum, G., Lister, G. S., Duboz, C., 2002. Relative motions of Africa, Iberia and Europe during Alpine orogeny. Tectonophysics 359(1-2), 117-129.

Sandwell, D. T., Yale, M. M., Smith, W. H. F., 1995. Gravity anomaly profiles from ERS-1, Topex and Geosat altimetry. Eos Trans. AGU 76(17), S89.

Saunders, A. D., Fornari, D. J., Morrison, M. A., 1982. The composition and emplacement of basaltic magmas produced during the development of continental-margin basins: the Gulf of California, Mexico. Journal of the Geological Society 139(3), 335-346.

Séranne, M., 1999. The Gulf of Lion continental margin (NW Mediterranean) revisited by IBS: an overview. Geological Society, London, Special Publications 156(1), 15-36

Shapiro, N. M., Campillo, M., Stehly, L., Ritzwoller, M. H., 2005. High-resolution surface-wave tomography from ambient seismic noise. Science 307(5715), 1615-1618.

Stehly, L., Fry, B., Campillo, M., Shapiro, N. M., Guilbert, J., Boschi, L., Giardini, D., 2009. Tomography of the Alpine region from observations of seismic ambient noise. Geophysical Journal International 178(1), 338-350.

Van Hinsbergen, D. J., Torsvik, T. H., Schmid, S. M., Maţenco, L. C., Maffione, M., Vissers, R. L., et al., 2020. Orogenic architecture of the Mediterranean region and kinematic reconstruction of its tectonic evolution since the Triassic. Gondwana Research 81, 79-229.

Terrinha, P., Pueyo, E. L., Aranguren, A., Kullberg, J. C., Kullberg, M. C., Casas-Sainz, A., Azevedo, M. D. R., 2018. Gravimetric and magnetic fabric study of the Sintra Igneous complex: laccolith-plug emplacement in the Western Iberian passive margin. International Journal of Earth Sciences 107, 1807-1833.

White, R. S., McKenzie, D., O'Nions, R. K., 1992. Oceanic crustal thickness from seismic measurements and rare earth element inversions. Journal of Geophysical Research: Solid Earth 97(B13), 19683-19715.

Wilson, D. S., Teagle, D. A., Alt, J. C., Banerjee, N. R., Umino, S., Miyashita, S., Ziegler, C., 2006. Drilling to gabbro in intact ocean crust. science, 312(5776), 1016-1020.

Wolf, F. N., Lange, D., Dannowski, A., Thorwart, M., Crawford, W., Wiesenberg, L., et al., 2021. 3D crustal structure of the Ligurian Basin revealed by surface wave tomography using ocean bottom seismometer data. Solid Earth 12(11), 2597-2613

Yan, F., Han, D. H., Yao, Q., Chen, X. L., 2016. Seismic velocities of halite salt: Anisotropy, heterogeneity, dispersion, temperature, and pressure effectsRock-physics properties of halite salt. Geophysics 81(4), D293-D301.

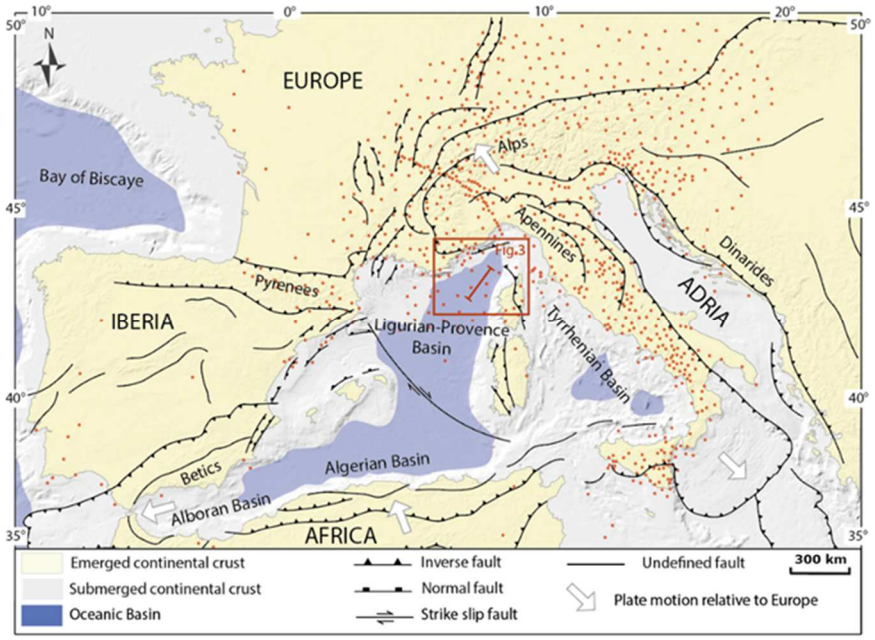

Figure 1 : Geodynamic map of the western Mediterranean with location of study area (red frame). Geodynamic context from Jolivet et al. (2020) and Facenna et al. (2014). Seismic stations from Nouibat et al. (2022a).

(1.5 column fitting image, colour printing)

Corresponding author:
E-mail address: louise.boschetti@get.omp.eu (L.Boschetti)

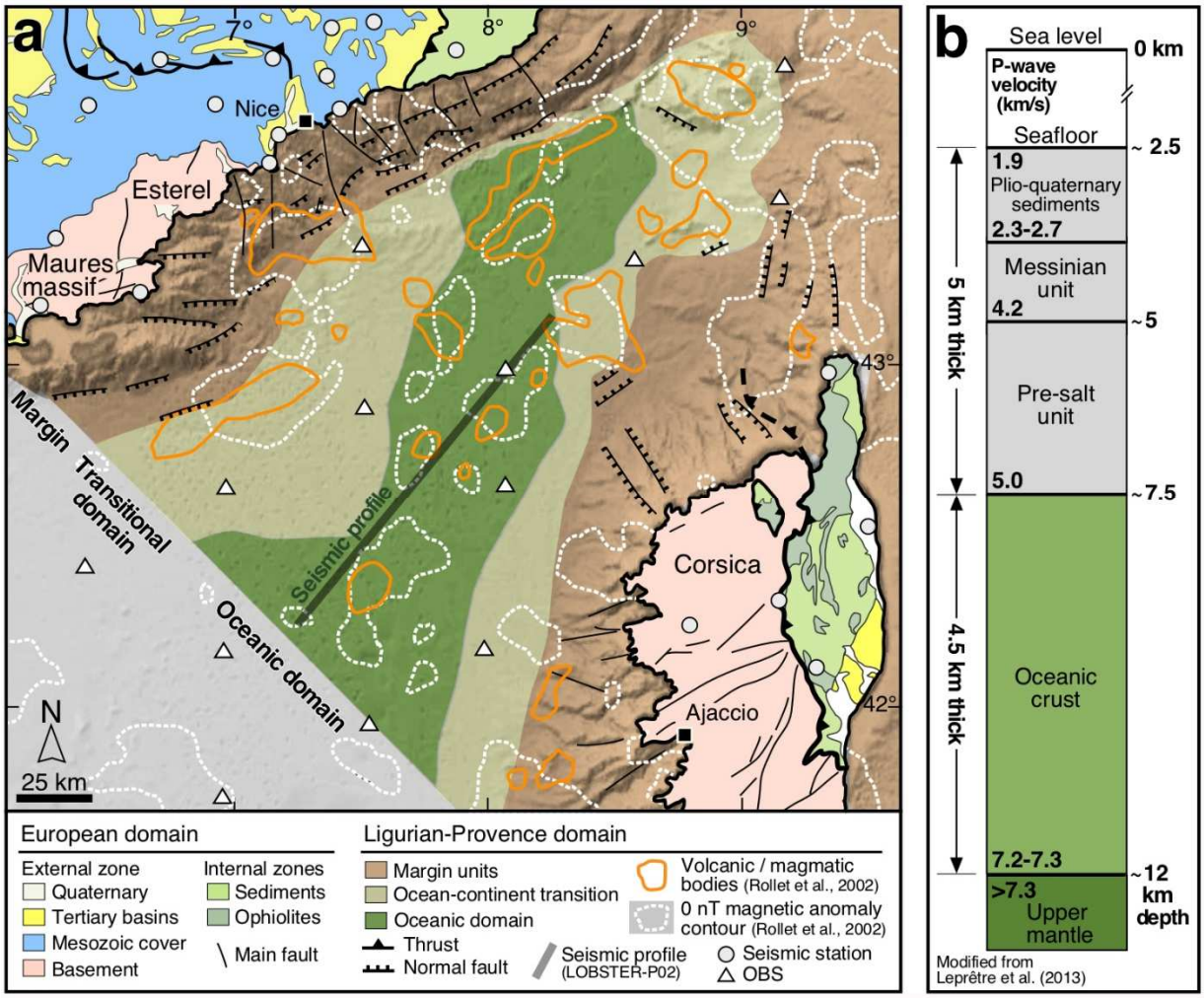

Figure 2 : a) Geological map of the Ligurian-Provencal basin modified from Nouibat et al. (2022a). Magnetic anomalies are taken from Rollet et al. (2002). (b) stratigraphic log showing P-wave velocities and thicknesses of geological units observed in Western Mediterranean basin (after Klingelhoefer et al., 2008; Gailler al., 2008; Leprêtre et al., 2013; Dannowski et al., 2020).

(2 column fitting image, colour printing)

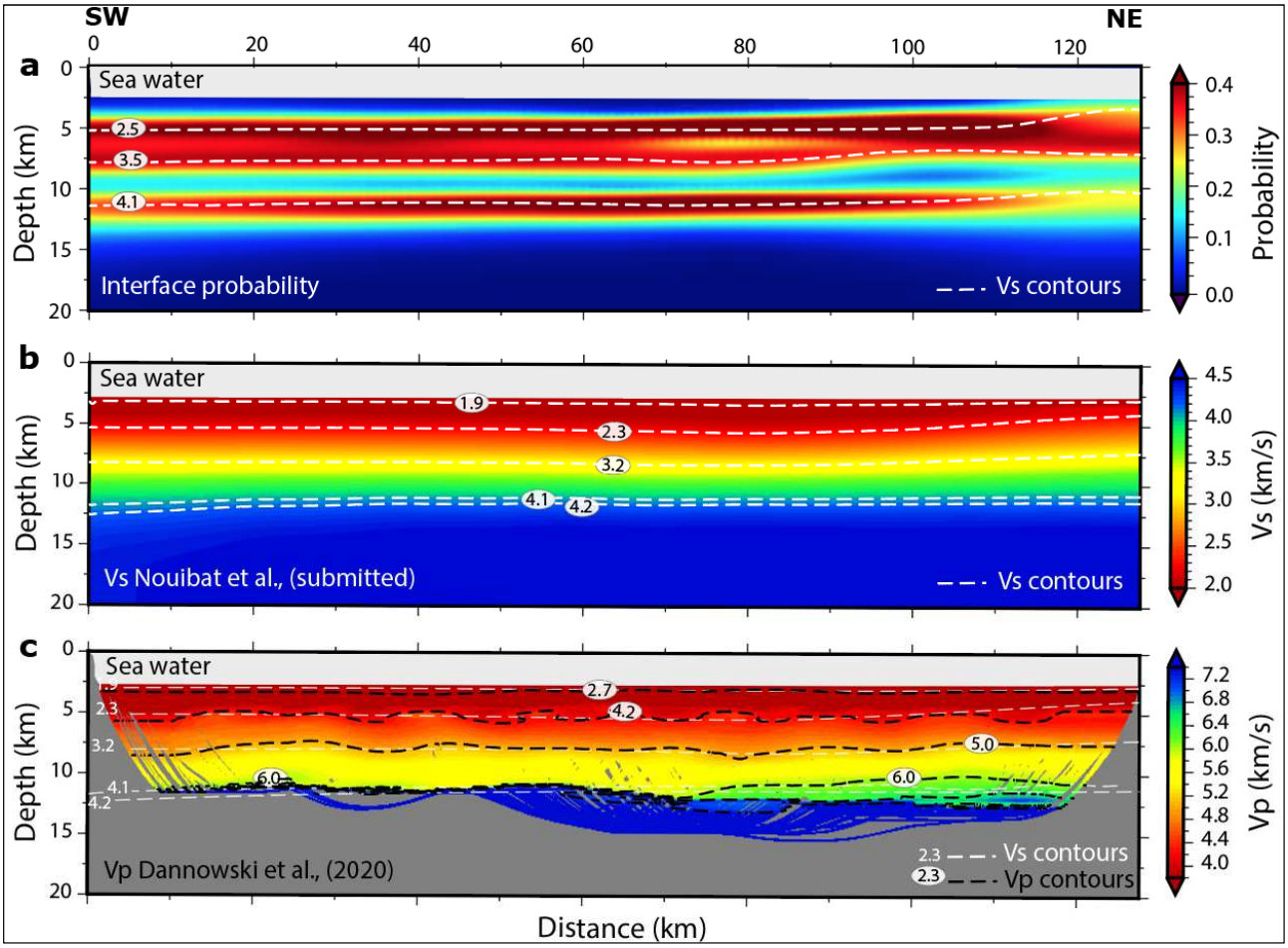

Figure 3 : Depth sections along the LOBSTER-P02 transect (location in Fig. 2); (a) Posterior probability densities of presence of a layer obtained from the Bayesian inversion. White dashed lines indicate Vs contours from (b). (b) Shear wave velocities from our final model. (c) P-wave velocities from Dannowski et al. (2020). Black dashed lines indicate Vp contours and white dashed lines as in (a).

(2 column fitting image, colour printing)

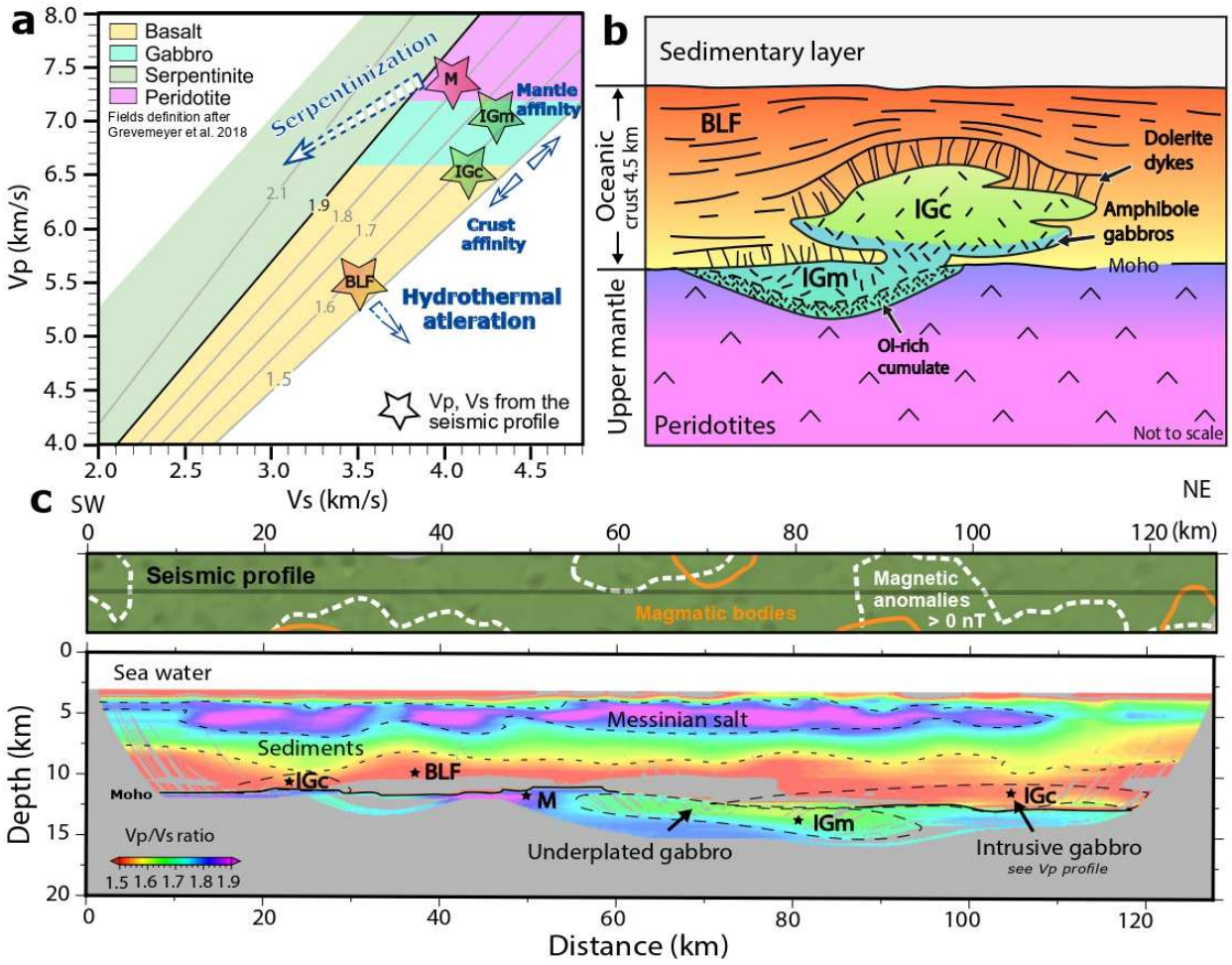

Figure 4 : Vp/Vs diagram modified from Grevemeyer et al. (2018). Stars represent domains where signals in Vp, Vs and Vp/Vs ratio are observed for each lithology. BFL: Basaltic Lava Flows; IGc; igneous gabbro with a crustal affinity; IGm: igneous gabbro with a mantle affinity; M: upper mantle. Blue arrows present possible evolution of the lithology. (b) Schematic interpretation based on results from (a). (c) Magnetic anomalies of LOBSTER-P02 transect from Rollet et al.,2002 (location Fig. 2) superimposed to the Vp/Vs ratio. Grey domains into the crust represent velocity values below 1.49, which are not coherent with crustal values. This local incoherence could result from discrepancies between the two different models with distinct resolutions. Black dashed lines represent possible contacts between lithologies. Back stars represent the lithologies defined in the diagram (a) above.

(2 column fitting image, colour printing)